Oct 26th, 12:00 AM

Computer Modeling of Sloped Z-purlin Supported Roof Systems to Predict Lateral Restraint Force Requirements

Michael W. Seek

Thomas M. Murray

Seventeenth International Specialty Conference on Cold-Formed Steel Structures
Orlando, Florida, U.S.A, November 4-5, 2004

Computer Modeling of Sloped Z-Purlin Supported Roof Systems to Predict Lateral Restraint Force Requirements

Michael W Seek, PE[1] and Thomas M Murray, Ph.D., PE[2]

Abstract

Lateral restraint or anchorage forces in Z-purlin supported through-fastened and standing seam (concealed clip) roof systems have been studied using the finite element method. Results from frame element models as well as full plate models are presented and compared to experimental results. Single and three span continuous systems with five restraint configurations were examined at roof slopes varying from zero to eighteen degrees from the horizontal. Recommendations for modification of existing anchorage force prediction equations are made.

Introduction

Z-Purlin supported roof systems have long been used by the metal building industry as a cost effective means of covering large roof systems. The development of standing seam systems has solved the thermal expansion and sealing problem of through-fastened systems. Their suitability in these applications has resulted in increased use as roof systems for conventional structures.

As a flexural member, the Z-purlin presents significant challenges from an analysis perspective. When an unrestrained Z-purlin is loaded in the plane of its web, it deflects laterally as well as vertically. Torsion is induced as a result of second order effects of the lateral displacement. Its stability is contingent upon

[1]Graduate Research Assistant, Virginia Tech, Blacksburg, VA, USA.
[2]Montague Betts Professor of Structural Steel Design, Virginia Tech, Blacksburg, VA, USA.

its attachment to the rafters, attachment to the roof sheathing and the application of external lateral restraint. Lateral restraint is typically applied in discrete locations along the length of a purlin.

Due to the many variables involved, the behavior of Z-purlin supported roof systems is difficult to accurately predict. A means of predicting lateral restraint forces is currently specified in the North American Specifications in Section D3.2.1 (AISI, 2003). It has been found from tests performed by Lee and Murray (2001) and the authors that the AISI equations can be overly conservative for low slope roofs and unconservative for roofs with large slopes.

In an effort to provide a reliable means of predicting lateral restraint, two computer models have been investigated. The first model with frame type finite elements had been developed previously by Elhouar and Murray (1985) and modified by Neubert and Murray (1999). It has been found that with further modifications to this model, good correlation to test results is realized. A second finite element model utilizing shell elements to represent the purlin and sheathing was also developed. It too has been shown to have good correlation with test results. The models will provide a means of modifying the lateral restraint force prediction equations proposed by Neubert and Murray (1999; Hancock, Murray, and Ellifritt, 2001) to allow for the direct calculation of lateral restraint forces.

Frame Finite Element Model

The frame element stiffness model used in the current analysis was first developed by Elhouar and Murray (1985). This model was correlated to full scale and quarter scale test results. Through regression analyses
of the model results, a series of parametric prediction equations was proposed and adopted by AISI. The equations, functions of purlin depth, thickness, flange width, and the number of purlins restrained, provide the basis for the current lateral restraint provisions specified in Section D3.2.1 of the North American Specifications (AISI 2003).

One important factor that the Elhouar and Murray (1985) study did not take into account is diaphragm stiffness. The frame element model was revisited by Neubert and Murray (1999) and modified to include variation of diaphragm panel stiffness. As a result of this work, a new methodology for the prediction of lateral restraint forces was proposed incorporating purlin cross sectional properties, diaphragm stiffness, and system effects. This prediction method is referred to as the Neubert and Murray Method.

The representation of the purlin used in these studies is shown in Figure 1. It is discretized into 12 segments along its length so that the third points, quarter points and midpoints all coincide with a node location. The purlin is comprised of Type A, B, C and F elements.

The Type A elements are the main components representing the purlin. The local X axis of the Type A element is oriented along the global X axis, but the member is rotated such that the local z and y axes correspond to the principal Y2 and X2 axes respectively as defined in the AISI Cold-Formed Steel Design Manual (1996). The section properties of the element correspond to the gross section properties of the purlin, i.e. Area = Area of the Purlin, $I_{zz} = I_{y2}$, $I_{yy} = I_{x2}$. To account for warping torsional stiffness and eliminate large torsional displacements, the torsional constant, J is set at an arbitrarily high value of 10 in^4.

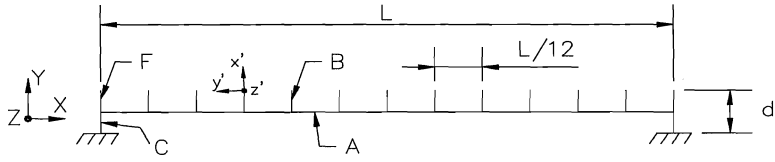

Figure 1. Model of Purlin in Frame Finite Element Model

Table 1. Frame Model Properties

Element Type	Model Area	Model Iyy	Model Izz	Model J
A	Area of Purlin	Ix2	Iy2	10
B	$\frac{Lt}{12}$	$\frac{Lt^3}{144}$	J	Ix2
C	$\frac{Lt}{2}$	$\frac{Lt^3}{24}$	J	Ix2
F	$\frac{Lt}{12}$	$\frac{Lt^3}{288}$	J	Ix2

Type B and F elements connect the Type A element with the roof sheathing and have properties corresponding to L/12 and L/24 of the purlin respectively. The local axes of these elements are denoted in Figure 1 by x′, y′ and z′. The most important property of these elements is the moment of inertia about the local y′ axis, I_{yy}. This property, in the case of the type B element, is the moment of inertia of a rectangular element with width equal to the tributary width of the element, L/12, and a height equal to the purlin thickness, t. The remaining properties of the Type B and F elements are denoted in Table 1.

Type C elements provide connection between the Type A element and the rafter supports and have the same local axes as the type B and F elements. A major departure from previous models is the treatment of the moment of inertia about the y-axis, I_{yy}. To eliminate excessive deformation of the type C element, Elhouar and Murray (1985) increased its moment of inertia twelve fold from that equivalent to a tributary width of L/2 to a value of:

$$I_{yy} = \frac{Lt^3}{2} \tag{1}$$

Neubert and Murray (1999) felt this value still resulted in excessive deflections and consequently underestimated restraint force results, so the value of I_{yy} was increased arbitrarily to 1 in^4 to eliminate all bending deformation about the y axis in the Type C element. In the current study, it was found that results closer to test results are realized if this value is reduced back to a value equal to the tributary width of the Type C element of L/2. The resulting value for the moment of inertia about the y-axis is then

$$I_{yy} = \frac{Lt^3}{24} \tag{2}$$

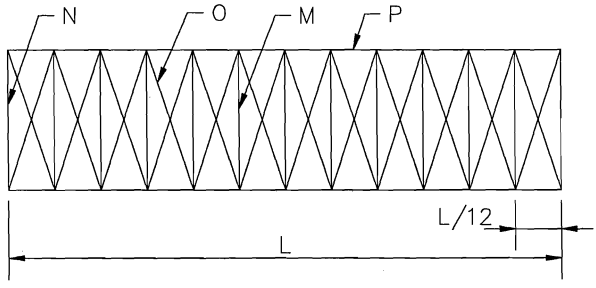

Figure 2 Diaphragm Elements

Figure 2 shows the "truss" diaphragm configuration used in this study. It follows the configuration used by both Elhouar and Murray (1988) and Neubert and Murray (1999) with some modification. The diaphragm is attached to the purlin at the top of the Type B and Type F elements. The diaphragm is comprised of type M, N, O and P elements, which are modeled as truss elements, i.e. bending stiffness about all axes is released and the element has only axial stiffness. The properties of these elements are derived from two stiffness sub-models. The first model, shown in Figure 3(a), is used to determine the cross sectional area of the diagonal type O elements, A_O, based on the desired diaphragm stiffness. Once the area of the Type O element is known, the second stiffness model, shown in figure 3(b), is solved for the area of the type N, M, and P elements, A_N, A_M, and A_P, respectively, to yield the true axial stiffness of the sheathing. Analyses of the models yields:

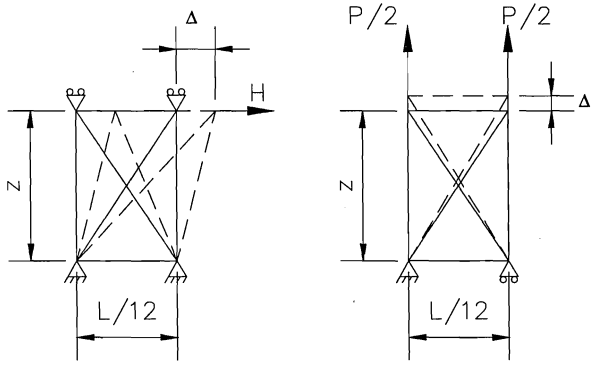

Figure 3. Cantilever Diaphragm Models

$$A_O = \frac{G' z(\alpha^2 + 1)^{3/2}}{2E\alpha^2} \tag{3}$$

$$A_N = \frac{\sqrt{b^2 + 4ac} - b}{2a} \tag{4}$$

$$A_M = 2A_N \tag{5}$$

$$A_P = \alpha A_N \tag{6}$$

where

$$a = 2zE\alpha\left(\alpha^2 + 1\right)^{3/2} \tag{7}$$

$$b = 2A_O zE(\alpha^4 + 1) - K_{axial} z^2 \alpha\left(\alpha^2 + 1\right)^{3/2} \tag{8}$$

$$c = K_{axial} A_O z^2 \tag{9}$$

$$\alpha = \frac{z}{\left(L/12\right)} \tag{10}$$

$$K_{axial} = \frac{A_{panel} E}{z} \tag{11}$$

and

z = Purlin Spacing c. to c. (in.)
L = Purlin Span (in.)
E = Modulus of Elasticity (ksi)
G' = Panel Diaphragm Stiffness (kip/in.)
A_{panel} = Panel Cross Sectional Area (in^2/ft panel width)

Previous applications of the diaphragm model in the Figure 2 model have used rigid supports for the immediate lateral restraints as shown in Figure 4 (a). In laboratory tests and actual field conditions, these restraints have a finite

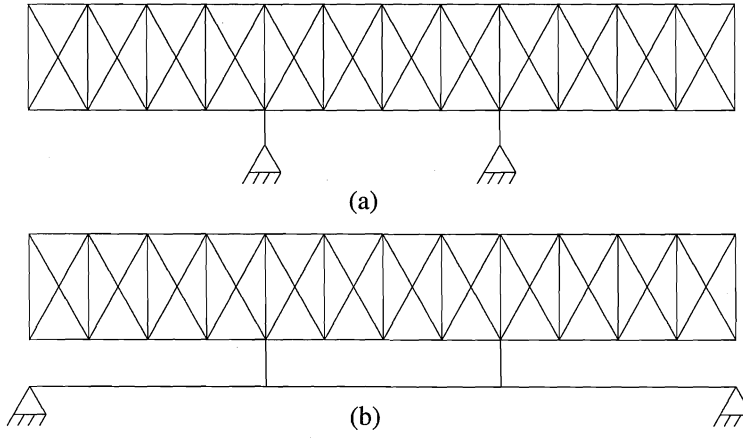

Figure 4. Restraint Anchorage

stiffness. Through analysis of the finite element models, Watson and Sears, (2003) discovered that variation of the stiffness of the lateral restraint can have a large effect on the restraint force. To simulate the stiffness of the restraints in laboratory tests, a beam of equal stiffness is modeled between rafter supports. Lateral restraints are attached to the beam along the purlin span as shown in Figure 4 (b). The connection between the diaphragm and beam is made by a type E element – a truss element with cross sectional area equivalent to a ½ in. diameter threaded rod as was used in the experimental tests.

In many standing seam roof systems, the clip connection between the purlin and standing seam sheathing incorporates a slider tab that allows the sheathing to move relative to the purlin to accommodate thermal expansion of the roof. To simulate this flexibility, the clip connection was modeled with a two node Link element. A Link element allows the user to define translational and rotational spring stiffness values between two nodes. The Link element is given a linear translational spring stiffness of 500 lb/in. in the direction parallel to the roof seams and perpendicular to the web of the purlin. This value was chosen because it gave the best correlation with test results.

Gravity loads are applied as uniformly distributed force along the Type A elements. The gravity force is divided into vertical and horizontal components according to the roof slope. The vertical force is w $\cos(\theta)$ and the horizontal force is w $\sin(\theta)$, where θ is the roof slope angle and w is the tributary linear load on each purlin. Because the vertical component of the gravity load is thought to act at an eccentricity of 1/3 the width of the top flange, an additional torque, T, is applied to the nodes at the top of the Type B and F elements,

$$T = w\cos(\theta) \times b/3 \times L/12$$

where b is the width of the purlin top flange.

Shell Finite Element Model

A plate element finite element model was developed using SAP 2000 Nonlinear V8, which has nonlinear capabilities. However, the analyses were restricted to linear, first order analyses. The model is comprised of two types of shell elements to represent the purlin and deck. The purlin is discretized into 2 in. segments along the length. A representation of the purlin is shown in Figure 5. The web is divided into four equal segments, the flange into three equal

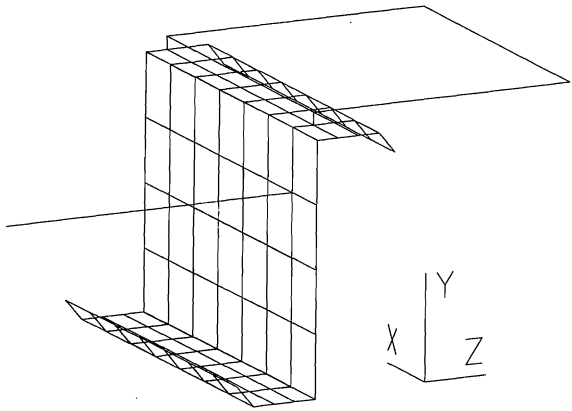

Figure 5. Shell Finite Element Model

segments, and each edge stiffener into a single element. The discretization was chosen so as to maintain a maximum four to one aspect ratio for all elements. Each element has a bending membrane thickness equal to the purlin thickness.

The sheathing panel is modeled with 12 in. along the length of the purlin by 10.8 in. between purlin elements. (10.8 in. x 5 panels = 54 in. purlin spacing). The membrane thickness of these elements is equivalent to the cross sectional area of the sheathing panel. To account for the bending stiffness provided by sheathing ribs, the bending stiffness of the element is equivalent to that of the deck, that is:

$$t_{sheathing} = \sqrt[3]{\frac{I_{sheathing}}{1\text{ in.}}} \qquad (13)$$

where $I_{sheathing}$ is the sheathing moment of inertia per foot of width.

To provide for variable panel shear stiffness, an orthotropic material was used, which allowed the shear modulus to be entered explicitly. Using a small model similar to the Cantilever Test for Diaphragms (*Cold-Formed* 1996), the shear modulus was adjusted until the desired panel shear stiffness was reached. Table 2 shows the panel diaphragm stiffness and respective shear modulus values used.

Table 2. Shell Diaphragm Properties

Panel Diphragm Stiffness (lb/in)	Shear Modulus (psi) (Based On Panel Membrane Thickness = 0.0197 in.)
500	2500
1000	50000
2500	115000
7500	297000
12500	442000
20000	617000
27500	775000

The attachment between the deck and the purlin is by a 2 node Link element. For the through fastened system models, the link represents the semi-rigid moment connection between the deck and purlin. Thus the link element has reduced stiffness for moment transfer between the purlin and deck about the Global X axis. The link attachment matched the fastener spacing of the laboratory test, that is, 12 in. For the standing seam models, the link element represented the standing seam clip attaching the sheathing to the purlin. The clip does not completely restrain rotation between the panel and purlin and many systems incorporate slider tabs that allow displacement between the sheathing and purlin. Therefore, for standing seam models, the link elements are spaced at 24 in. intervals to match clip spacing and are given translational spring stiffness in the global Y and rotational spring stiffness about the global X axis. The link element attaches the sheathing to the purlin at a distance of 1/3 of the flange width.

Load is applied directly to the sheathing as a uniformly distributed area load in both the global Y direction (gravity) and the global Z direction (downslope). To account for roof slope, the load in the global Y direction is equal to U cos(θ) and in the global Z direction is equal to U sin (θ), where U is the uniformly distributed load and θ is the roof slope.

At each simulated rafter support location, the purlin is restrained against translation in the Global Y and Z directions as well as rotation about the Global X axis. This restraint is applied at a discrete point at the centerline of the rafter support at the base of the purlin web.

The lateral restraint is applied in a similar manner as the frame element models. To match test specimens, the lateral restraints, modeled as a truss elements with

the cross sectional area of a ½ in. diameter rod, are attached to the web of the purlin 2 ½ in. below the top of the purlin. Rather than attaching these restraint rods to a rigid support, a beam representing the test specimen was modeled similar to Figure 4 (b).

Comparison of Finite Element Models with Laboratory Test Results

To test the validity of the anchorage force prediction current equations in Section D3.2.1 of the North American Specification, the method proposed by Neubert and Murray (1999), and the modified finite element models, a series of full scale laboratory tests was performed. The tests were performed using 10Z2.6x0.097 purlins spaced at 54 in. center to center. The purlins spanned 20 ft for the single span tests and three 20 ft spans for the multiple span tests. For the multiple span cases, the purlins were lapped a total of 6 ft centered over the rafter. The tests included combinations of two, four, and six purlins on single spans and six purlins lines over multiple spans. Each of these combinations was tested using conventional through fastened sheathing and standing seam sheathing and clips with slider tabs. The test apparatus permitted variation in slope from zero to a 4:12 pitch. For each purlin arrangement and bracing configuration, the test specimen was loaded uniformly to approximately 20 psf. Six anchorage force measurements at incremental slopes between 0 and 4:12 were taken. Five different anchorage configurations were investigated: Supports, 3rd Points, Midpoints, Quarter Points and 3rd Points + Supports.

For virtually all combinations of purlins and restraint configurations, the North American specification equations give poor correlation with the test results. The results are typically highly conservative for low slope roofs but tend to be unconservative for roof pitches above 2:12.
The prediction method proposed by Neubert and Murray (1999) resulted in better correlation than the North American Specification method. Considering the Supports, 3rd Points and Midpoint restraint configuration on single span systems, the Neubert and Murray method shows good correlation but deviates slightly with increasing number of purlin lines. For Quarter points and 3rd Points + Supports configurations, the Neubert and Murray method does not very well correlate with the test results. A similar trend is observed for the multiple span configurations.

With the modifications made to the frame element models outlined in this article, improved correlation with the test results is realized. The improvement is minor when considering Supports, 3rd points and midpoints restraints because

the correlation with the Neubert and Murray method is already fairly good. The improvement is particularly noticeable when considering the 3rd points + Supports and Quarter Points cases. However, for the quarter points restraint using through fastened deck, the results begin to deviate quite dramatically as the number of purlin lines is increased.

The correlation between the test results and the plate finite element models is very good for virtually all test cases. The through fastened cases show the best correlation. The standing seam models show some slight deviation from the test results but still provide a fairly accurate means of predicting restraint forces. The plate finite element model seems to be very stable and less susceptible to slight changes in the model than the frame finite element model. However for large systems of multiple spans with 6 or more purlin lines, run times with the plate finite element model approach 1 hour, while the run time for an equivalent frame finite element model is virtually instantaneous.

Conclusions

Progress has been made towards better predicting the anchorage forces requirements in standing seam roof systems. Modifications have been made to the frame finite element model that was used to develop both the equations in Section D3.2.1 of the North American specifications and the Neubert and Murray Method. Modifications to this model have improved the correlation to test results. Additionally a plate finite element model has been developed that too shows good correlation to test results. It is felt that with improvement to the finite element models, improvements to the Neubert and Murray Method can be made to provide an accurate means of directly calculating the required restraint forces in Z-purlin supported roof systems.

Appendix – References

Cold-Formed Steel Design Manual, (1996). American Iron and Steel Institute, Washington, D.C.

Elhouar , S. and Murray, T.M. (1985). "Prediction of Lateral Restraint Forces for Z-purlin Supported Roof Systems." Fears Structural Engineering Laboratory Report No. FSEL/AISI85-01, University of Oklahoma, Norman Oklahoma, 107 Pages.

Hancock, G. J., Murray, T. M. and Ellifrit, D. S. (2001). *Cold-Formed Steel Structures to the AISI Specification*, Marcel Dekker, New York.

Neubert, M.C. and Murray, T.M. (1999). "Estimation of Required Restraint Forces in Z-purlin Supported, Sloped Roofs Under Gravity Loads." Research Report CE/VPI-ST-99/12. Department of Civil and Environmental Engineering, Virginia Polytechnic Institute and State University, Blacksburg, VA, 112 Pages.

Lee, S.L. and Murray, T.M. (2001). "Experimental Determination of Required Lateral Restraint Forces for Z-Purlin Supported, Sloped Metal Roof Systems." Research Report CE/VPI-ST-01/09. Department of Civil and Environmental Engineering, Virginia Polytechnic Institute and State University, Blacksburg, VA, 104 Pages.

North American Specification for the Design of Cold-Formed Steel Structural Memebers (2003). American Iron and Steel Institute. Washington, D.C.

Watson, D and Sears, J. (2003). *Progress on Lateral Restraint Forces.* Private Correspondence, September 23.

Appendix – Notation

A_{panel} = Panel cross sectional area (in^2/ft panel width)
A_M = Area of Type M element (in^2)
A_N = Area of Type N element (in^2)
A_O = Area of Type O element (in^2)
A_P = Area of Type P element (in^2)
E = Modulus of elasticity (ksi)
G' = Panel diaphragm stiffness (kip/in.)
$I_{Sheathing}$ = Moment of inertia of roof sheathing per foot width (in^4/ft)
I_{X2} = Minor principal axis moment of inertia (in^4)
I_{YY} = Moment of inertia about local y axis (in^4)
I_{Y2} = Major principal axis moment of inertia (in^4)
I_{ZZ} = Moment of inertia about local z axis (in^4)
L = Purlin span (in.)
T = Torque due to dccentric loading on purlin flange (Lb-in)
$T_{sheathing}$ = Equivalent bending thickness of roof sheathing (in.)
U = Total uniformly distributed gravity load (psf)
w = Tributary line load on purlin (plf)
z = Purlin spacing center to center (in.)
θ = Roof slope angle (degrees)